To print higher-resolution math symbols, click the **Hi-Res Fonts for Printing** button on the jsMath control panel. If the math symbols print as black boxes, turn off **image alpha channels** using the **Options** pane of the jsMath control panel.

The HI 21 cm Line

Hydrogen is the most abundant element in the interstellar medium (ISM), but the symmetric H_2 molecule has no permanent dipole moment and hence does not emit a detectable spectral line at radio frequencies. Neutral hydrogen (HI) atoms are abundant and ubiquitous in low-density regions of the ISM. They are detectable in the $\lambda \approx 21$ cm ($\nu_{10} = 1420.405751\ldots$ MHz) ***hyperfine line***. Two energy levels result from the magnetic interaction between the quantized electron and proton spins. When the relative spins change from parallel to antiparallel, a photon is emitted.

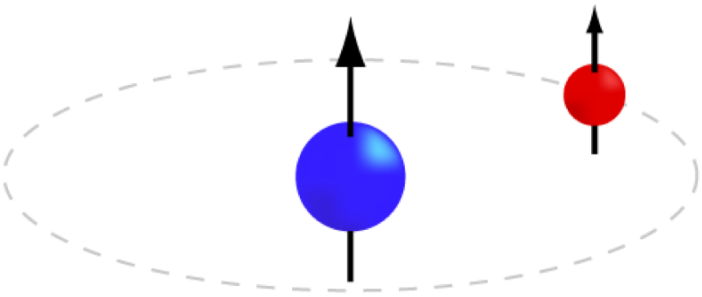

One $\lambda = 21$ *cm photon is emitted when the spins flip from parallel to antiparallel.* *Image credit*

The line center frequency is

$$\nu_{10} = \frac{8}{3} g_{\rm I} \left(\frac{m_{\rm e}}{m_{\rm p}}\right) \alpha^2 (R_{\rm M} c) \approx 1420.405751 \text{ MHz} \quad (7E1)$$

where $g_{\rm I} \approx 5.58569$ is the ***nuclear g-factor*** for a proton, $\alpha \equiv e^2/(\hbar c) \approx 1/137.036$ is the dimensionless ***fine-structure constant***, and $R_{\rm M} c$ is the hydrogen Rydberg frequency (Eq. 7A2).

$$\nu_{10} \approx \frac{8}{3} \cdot 5.58569 \cdot \left(\frac{1}{1836.12}\right) \left(1/137.036\right)^2 \cdot 3.28984 \times 10^{15} \text{ Hz} \left(1 + \frac{1}{1836.12}\right)^{-1}$$

$$\nu_{10} \approx 1420.4 \text{ MHz}$$

By analogy with the emission coefficient of radiation by an electric dipole

$$A_{\rm UL} \approx \frac{64\pi^4}{3hc^3} \nu_{\rm UL}^3 |\mu_{\rm UL}|^2 \ ,$$

the emission coefficient of this magnetic dipole is

$$A_{\rm UL} \approx \frac{64\pi^4}{3hc^3} \nu_{\rm UL}^3 |\mu_{10}^*|^2 \ ,$$

where μ_{10}^* is the mean magnetic dipole moment for HI in the ground electronic state ($n = 1$). The magnitude $|\mu_{10}|$ equals the ***Bohr magneton***, the intrinsic dipole moment of an electron. Electrons

have spin angular momentum $L = \hbar/2$, classical radius $r_e = e^2/(m_e c^2)$, and charge e, so

$$|\mu_{10}^*| = \frac{\hbar}{2}\frac{e}{m_e c} \approx \frac{6.63 \times 10^{-27}\ \text{erg s}/(2\pi)}{2} \cdot \frac{4.8 \times 10^{-10}\ \text{statcoul}}{9.11 \times 10^{-28}\ \text{g} \cdot 3 \times 10^{10}\ \text{cm s}^{-1}}$$

$$|\mu_{10}^*| \approx 9.27 \times 10^{-21}\ \text{erg Gauss}^{-1}$$

Thus the emission coefficient of the 21 cm line is

$$A_{10} \approx \frac{64\pi^4 (1.42 \times 10^9\ \text{Hz})^3}{3 \cdot 6.63 \times 10^{-27}\ \text{erg s}\ (3 \times 10^{10}\ \text{cm s}^{-1})^3} (9.27 \times 10^{-21}\ \text{erg Gauss}^{-1})^2$$

$$\boxed{A_{10} \approx 2.85 \times 10^{-15}\ \text{s}^{-1}} \quad \text{(7E2)}$$

That is, the radiative half-life of this transition is about

$$\tau_{1/2} = A_{10}^{-1} \approx 3.5 \times 10^{14}\ \text{s} \approx 11\ \text{million years}$$

Such a low emission coefficient implies an extremely low critical density (defined by Eq. 7D10) $n^* \ll 1\ \text{cm}^{-3}$, so collisions can easily maintain this transition in LTE throughout the diffuse interstellar medium of a normal galaxy.

Regardless of whether the HI is in LTE or not, we can define the HI ***spin temperature*** T_s (the HI analog of the molecular excitation temperature T_x defined by Equation 7B8) by

$$\boxed{\frac{N_1}{N_0} \equiv \frac{g_1}{g_0} \exp\left(-\frac{h\nu_{10}}{kT_s}\right)}, \quad \text{(7E3)}$$

where the statistical weights of the upper and lower spin states are $g_1 = 3$ and $g_0 = 1$, respectively. Note that

$$\frac{h\nu_{10}}{kT_s} \approx \frac{6.63 \times 10^{-27}\ \text{erg s} \cdot 1.42 \times 10^9\ \text{Hz}}{1.38 \times 10^{-16}\ \text{erg K}^{-1} \cdot 150\ \text{K}} \approx 5 \times 10^{-4} \ll 1$$

is very small for gas in LTE at $T \approx T_s \approx 150$ K, so in the ISM

$$\frac{N_1}{N_0} \approx \frac{g_1}{g_0} = 3 \qquad \text{and} \qquad N_H = N_0 + N_1 \approx 4N_0$$

Inserting these weights into Equation 7B7 for the opacity coefficient of the $\lambda = 21$ cm line gives

$$\kappa_\nu = \frac{c^2}{8\pi\nu_{10}^2}\frac{g_1}{g_0} N_0 A_{10} \left[1 - \exp\left(-\frac{h\nu_{10}}{kT_s}\right)\right] \phi(\nu)$$

$$\kappa_\nu \approx \frac{c^2}{8\pi\nu_{10}^2} \cdot 3 \cdot \frac{N_H}{4} A_{10} \left(\frac{h\nu_{10}}{kT_s}\right) \phi(\nu)$$

$$\kappa_\nu \approx \frac{3c^2}{32\pi}\frac{A_{10}N_{\rm H}}{\nu_{10}}\frac{h}{kT_{\rm s}}\phi(\nu) \quad (7E4)$$

where $N_{\rm H}$ is the number of neutral hydrogen atoms per cm^3. The neutral hydrogen ***column density*** along any line-of-sight is defined as

$$\eta_{\rm H} \equiv \int_{\rm los} N_{\rm H}(s)ds \quad (7E5)$$

The total opacity τ of isothermal HI is proportional to the column density. If $\tau \ll 1$, then the integrated HI emission-line brightness $T_{\rm b}$ is proportional to the column density of HI and is independent of the spin temperature $T_{\rm s}$ because $T_{\rm b} \approx T_{\rm s}\tau$ and $\tau \propto T_{\rm s}^{-1}$ in the radio limit $h\nu_{10}/(kT_{\rm s}) \ll 1$. Thus $\eta_{\rm H}$ can be determined directly from the integrated line brightness when $\tau \ll 1$. In astronomically convenient units it can be written as

$$\left(\frac{\eta_{\rm H}}{\rm cm^{-2}}\right) \approx 1.82\times10^{18}\int\left[\frac{T_{\rm b}(v)}{\rm K}\right]d\left(\frac{v}{\rm km\ s^{-1}}\right) \quad (7E6)$$

where $T_{\rm b}$ is the observed 21 cm line brightness temperature at radial velocity v and the velocity integration extends over the entire 21 cm line profile. Note that *absorption* by HI in front of a continuum source with continuum brightness temperagure $> T_{\rm s}$, on the other hand, is weighted in favor of colder gas.

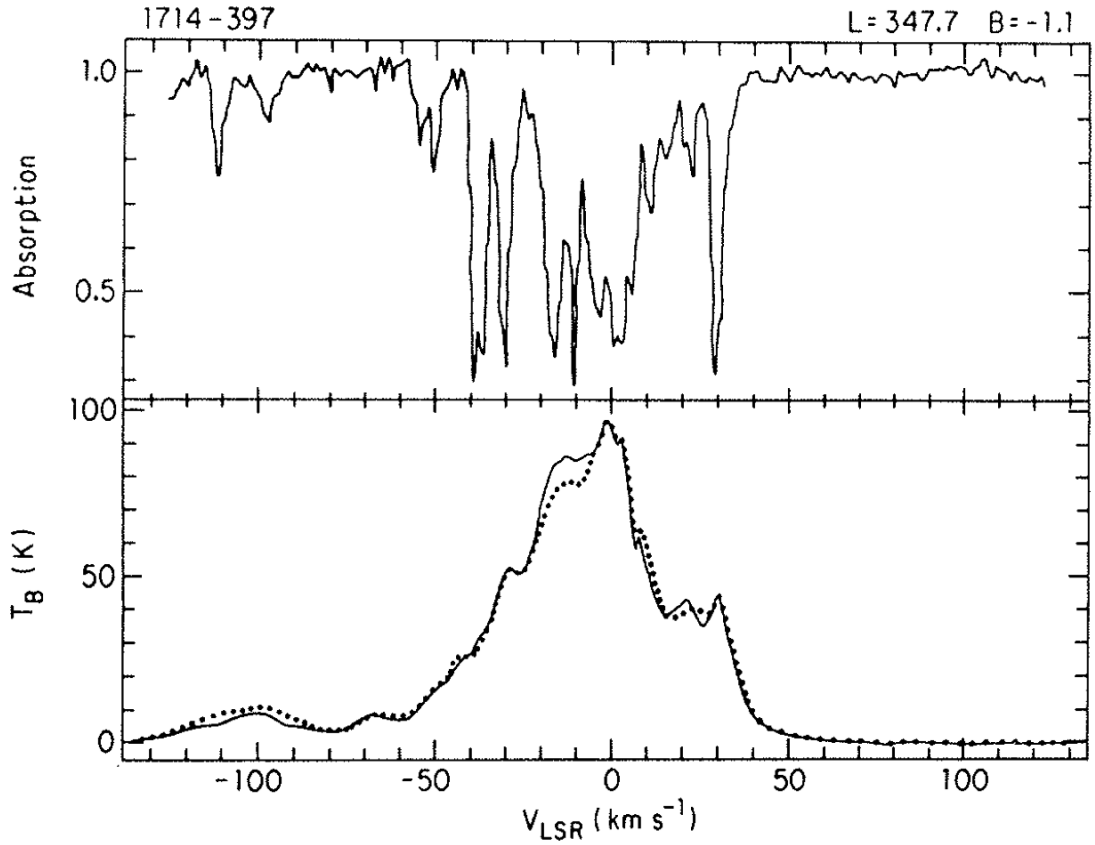

The HI absorption and emission spectra toward the source 1714-397 (Dickey, J. M. et al. 1983, ApJS, 53, 591).

The equilibrium temperature of cool interstellar HI is determined by the balance of heating and cooling. The primary heat sources are cosmic rays and ionizing photons from hot stars. The main coolant in the cool ISM is radiation from the fine-structure line of singly ionized carbon, CII, at $\lambda = 157.7\ \mu$m. This line is strong only when the temperature is at least

$$kT \approx h\nu = \frac{hc}{\lambda},$$

so the cooling rate increases exponentially above

$$T \approx \frac{hc}{k\lambda} \approx \frac{6.63 \times 10^{-27}\ \mathrm{erg\,s} \cdot 3 \times 10^{10}\ \mathrm{cm\,s^{-1}}}{1.38 \times 10^{-16}\ \mathrm{erg\,K^{-1}} \cdot 157.7 \times 10^{-4}\ \mathrm{cm}} \approx 91\ K\ .$$

The actual kinetic temperature of HI in our Galaxy can be estimated from the HI line brightness temperatures in directions where the line is optically thick ($\tau \gg 1$) and the brightness temperature approaches the excitation temperature, which is close to the kinetic temperature in LTE. Many lines-of-sight near the galactic plane have brightness temperatures as high as 100 150 K, values consistent with the temperature-dependent cooling rate.

Galactic HI

Neutral hydrogen gas in the disk of our Galaxy moves in nearly circular orbits around the galactic center. Radial velocities $V_{\rm r}$ measured from the Doppler shifts of HI $\lambda = 21$ cm emission lines encode information about the ***kinematic distances*** d of HI clouds, and the spectra of HI absorption in front of continuum sources can be used to constrain their distances also. HI is optically thin except in a few regions near the galactic plane, so the distribution of hydrogen maps out the large-scale structure of the whole Galaxy, most of which is hidden by dust at visible wavelengths.

The figure below shows a plan view of the galactic disk. The Sun ($\odot$) lies in the disk and moves in a circular orbit around the galactic center. The distance to the galactic center $R_\odot = 8.0 \pm 0.5$ kpc and the Sun's orbital speed $\omega_\odot R_\odot \approx 220$ km s^{-1} have been measured by a variety of means (Reid, M. J. 1993, ARAA, 31, 345). All HI clouds at galactocentric distance R are assumed to be in circular orbits with angular velocity $\omega(R)$, where $\omega(R)$ is a monotonically decreasing function of R. For cloud 1 at galactocentric azimuth θ on the line of sight at galactic longitude l, the observed radial velocity $V_{\rm r}$ relative to the Sun is given by

$$V_{\rm r} = \omega R \cos[\pi/2 - (l + \theta)] - \omega_\odot R_\odot \cos(\pi/2 - l)$$

Using the trigonometric identities $\cos[\pi/2 - (l + \theta)] = \sin(l + \theta)$ and $\sin(l + \theta) = \sin\theta\cos l + \cos\theta\sin l$ we obtain

$$V_{\rm r} = \omega R(\sin\theta\cos l + \cos\theta\sin l) - \omega_\odot R_\odot \sin l$$

$$V_{\rm r} = R_\odot(\omega - \omega_\odot)\sin l$$

To apply this equation, we need to determine the rotation curve $R\omega(R)$. The maximum radial velocity on the line of sight at longitude l is called the "terminal velocity" $V_{\rm T}$. Since ω decreases with R, this velocity occurs at the minimum $R = R_{\rm min} = R_\odot \sin l$ where the orbit is tangent to the line of sight:

$$V_{\rm T} = R_\odot[\omega(R_{\rm min}) - \omega_\odot]\sin l$$

We can determine the rotation curve from measurements of V_T spanning a wide range of l and thus of R_{min}.

Example: At galactic longitude $l = 30°$, the terminal velocity is observed to be $V_T \approx 130$ km s^{-1}. What is R_{min} and the orbital speed $R_{min}\omega(R_{min})$?

$$R_{min} = R_\odot \sin l = 8.0 \text{ kpc} \cdot 0.5 = 4.0 \text{ kpc}$$

$$V_T = R_\odot[\omega(R_{min}) - \omega_\odot]\sin l$$

$$V_T = R_{min}\omega(R_{min}) - R_\odot\omega_\odot \sin l$$

$$R_{min}\omega(R_{min}) = V_T + R_\odot\omega_\odot \sin l$$

$$R_{min}\omega(R_{min}) = 130 \text{ km s}^{-1} + 220 \text{ km s}^{-1} \times 0.5 = 240 \text{ km s}^{-1}$$

Note that, for $|l| < \pi/2$, there is a distance ambiguity: clouds 1 and 2 both have the same radial velocities but different distances d. There is no distance ambiguity for $|l| > \pi/2$.

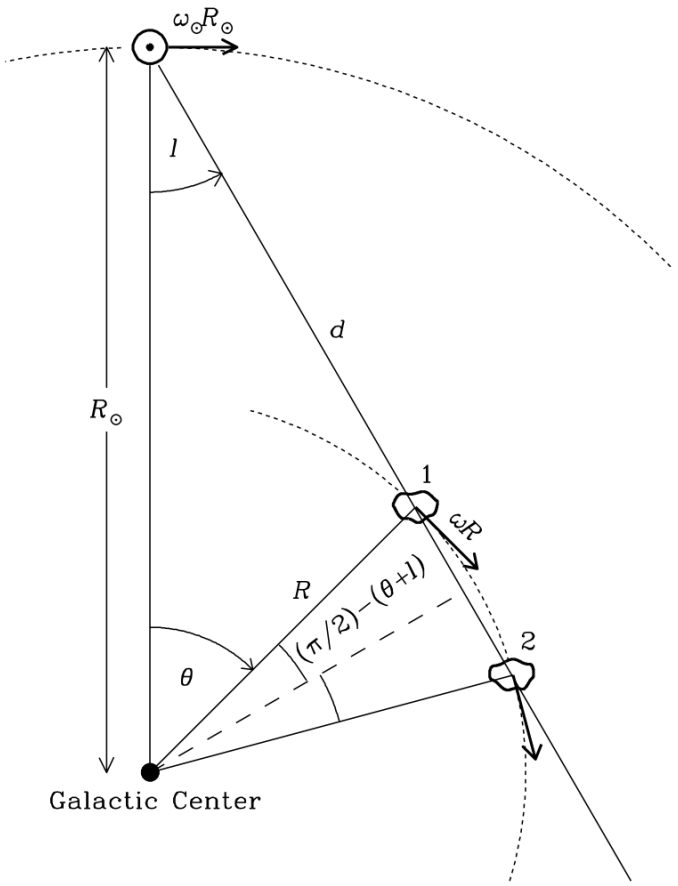

In the simplest realistic model for the galactic disk, the Sun and all HI clouds are in circular orbits about the Galactic Center, and the angular orbital velocity ω is a monotonically decreasing function of the orbital radius R. The distance of the Galactic Center is $R_\odot = 8.0 \pm 0.5$ kpc, and the Sun's orbital speed is $\omega_\odot R_\odot \approx 220$ km s^{-1}. For $|l| < \pi/2$, two HI clouds (1 and 2) can have the same radial velocity but be at different distances from the Sun.

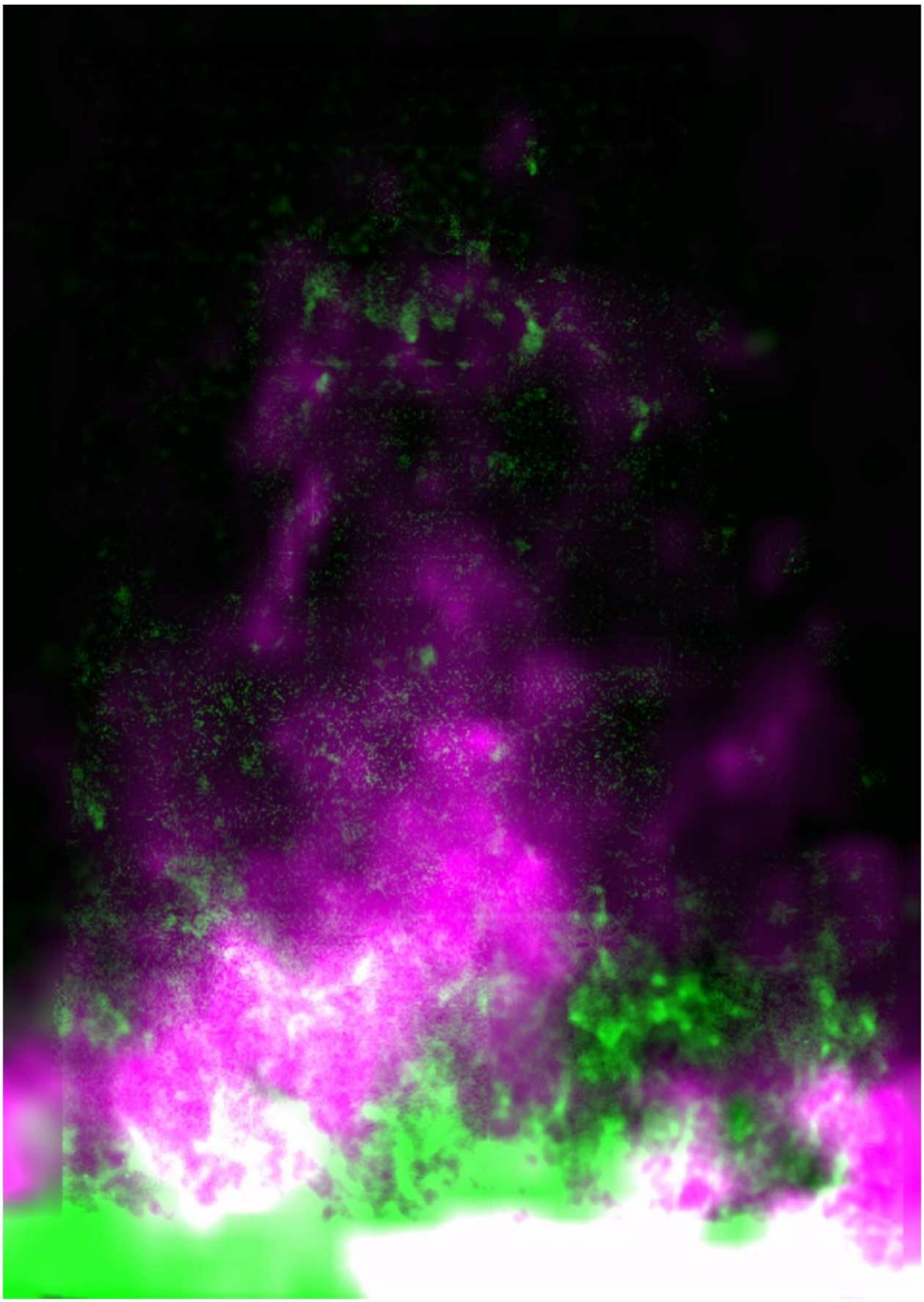

This image shows a galactic "superbubble" in HI (green) and HII (purple) about 7 kpc distant and 3 kpc in height. Stellar winds and supernovae in young star clusters blow these bubbles. Images of HI away from the galactic plane are easily contaminated by sidelobe responses to the strong and widespread HI emission from the plane itself. The low sidelobe levels of the clear-aperture GBT make such HI images possible. *Image credit*

HI in External Galaxies

The 1420 MHz HI line is an extremely useful tool for studying gas in the ISM of external galaxies and tracing the large-scale distribution of galaxies in the universe because HI is detectable in most spiral galaxies and in some elliptical galaxies.

The observed center frequency of the HI line can be used to measure the radial velocity V_r of a galaxy. The radial velocity of a galaxy is the sum of the recession velocity caused by the uniform Hubble expansion of the universe and the "peculiar" velocity of the galaxy. The radial component of the peculiar velocity reflects motions caused by gravitational interactions with nearby galaxies and is typically ~ 200 km s^{-1} in magnitude. The Hubble velocity is proportional to distance from the Earth, and the ***Hubble constant*** of proportionality has been measured as $H_0 \approx 72$ km s^{-1} Mpc^{-1}. If the radial velocity is significantly larger than the radial component of the peculiar velocity, the observed HI frequency can be used to estimate the ***Hubble distance*** $D \approx v_r/H_0$ to a galaxy.

Example: Use the HI emission-line profile below of the galaxy UGC 11707 to estimate its Hubble distance
$D \approx v_r/H_0$ if $H_0 \approx 72$ km s^{-1} Mpc^{-1}. If the radial velocity $v_r \ll c$, then the nonrelativistic Doppler formula can be used to calculate v_r from the observed line frequency ν:

$$\frac{v_r}{c} \approx \frac{\nu_0 - \nu}{\nu_0} ,$$

where $\nu_0 \approx 1420.4$ MHz is the rest-frame frequency. This equation yields what is known as the ***radio velocity*** because radio astronomers measure frequencies, not wavelengths. Optical astronomers measure wavelengths, not frequencies, so the ***optical velocity*** is defined by

$$\frac{v_r}{c} \approx \frac{\lambda - \lambda_0}{\lambda_0} .$$

Beware of this "gotcha": the optical and radio velocities are not exactly equal. Occasionally an observer confuses them, fails to center the observing passband on the correct frequency, and ends up with only part of the HI spectrum of a galaxy.

Since $\lambda = 21$ cm is such a long wavelength, many galaxies are unresolved by single-dish radio telescopes. For example, the half-power beamwidth of the 100 m GBT is about 9 arcmin at $\lambda = 21$ cm. Thus a single pointing is sufficient to obtain a spectral line representing all of the HI in any but the nearest galaxies.

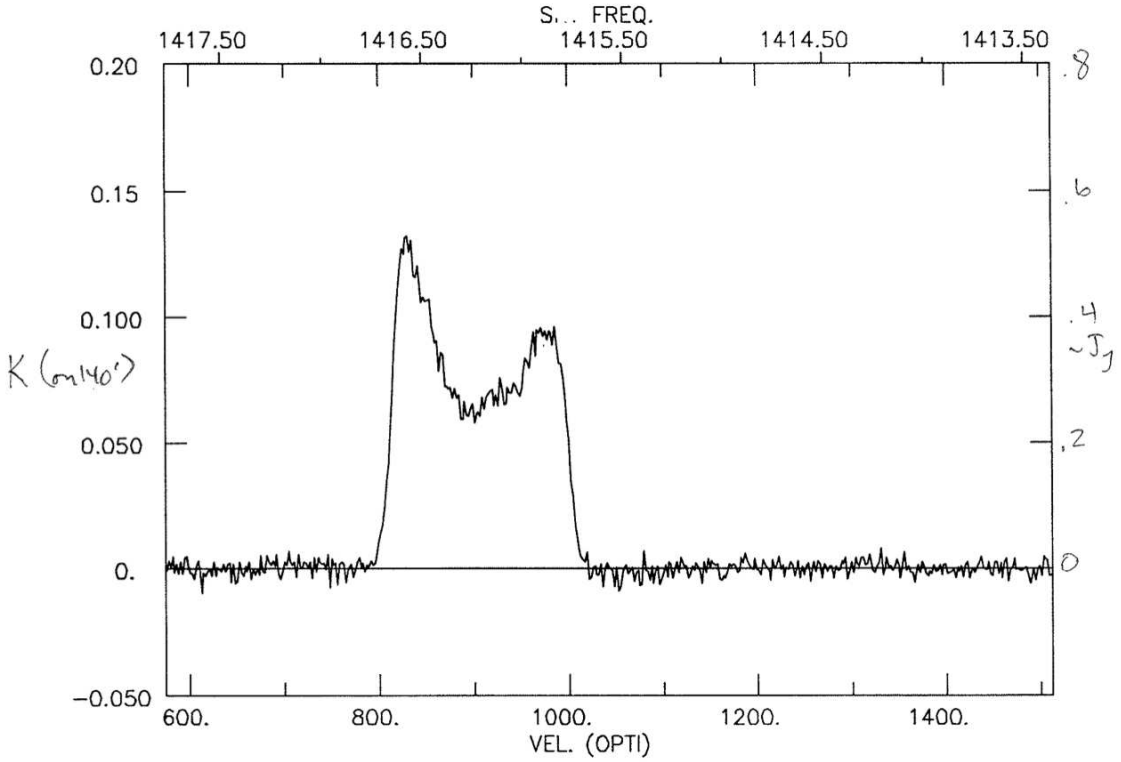

This integrated HI spectrum of UGC 11707 obtained with the 140-foot telescope (beamwidth ≈ 20 arcmin) shows the typical two-horned profile of a spiral galaxy.

For UGC 11707, the line center frequency is $\nu \approx 1416.2$ MHz, so

$$v_{\rm r} \approx c\left(1-\frac{\nu}{\nu_0}\right) \approx 3\times 10^5 \ {\rm km\ s^{-1}} \left(1-\frac{1416.2\ {\rm MHz}}{1420.4\ {\rm MHz}}\right) \approx 890\ {\rm km\ s^{-1}}$$

$$D \approx \frac{v_{\rm r}}{H_0} = \frac{890\ {\rm km\ s^{-1}}}{72\ {\rm km\ s^{-1}\ Mpc^{-1}}} = 12.4\ {\rm Mpc}$$

If the HI emission from a galaxy is optically thin, then the integrated line flux is proportional to the mass of HI in the galaxy, independent of the unknown HI temperature. It is a straightforward excercise to derive from Equation 7E6 the relation

$$\left(\frac{M_{\rm H}}{M_\odot}\right) \approx 2.36\times 10^5 \left(\frac{D}{\rm Mpc}\right)^2 \int \left[\frac{S(v)}{\rm Jy}\right]\left(\frac{dv}{\rm km\ s^{-1}}\right) \quad (7E7)$$

for the total ***HI mass*** $M_{\rm H}$ of a galaxy. The integral $\int S(v)dv$ over the line is called the ***line flux*** and is usually expressed in units of Jy km s^{-1}.

Example: What is the HI mass of UGC 11707?

We assume $\tau \ll 1$. The single-dish profile of UGC 11707 above indicates a line flux

so

$$\int S(v)\,dv \approx 0.35 \text{ Jy } \times 200 \text{ km s}^{-1} \approx 70 \text{ Jy km s}^{-1}$$

$$\left(\frac{M_{\rm H}}{M_\odot}\right) \approx 2.36 \times 10^5 \cdot (12.4)^2 \cdot 70 \approx 2.5 \times 10^9$$

Small statistical corrections for nonzero τ can be made from knowledge about the expected opacity as a function of disk inclination, galaxy mass, morphological type, etc.

A well-resolved HI image of a galaxy yields the ***total mass*** $M(r)$ enclosed within radius r of the center if the gas orbits in circular orbits. Circular orbits yield a characteristic radial velocity field, illustrated by nearby spiral galaxy M33.

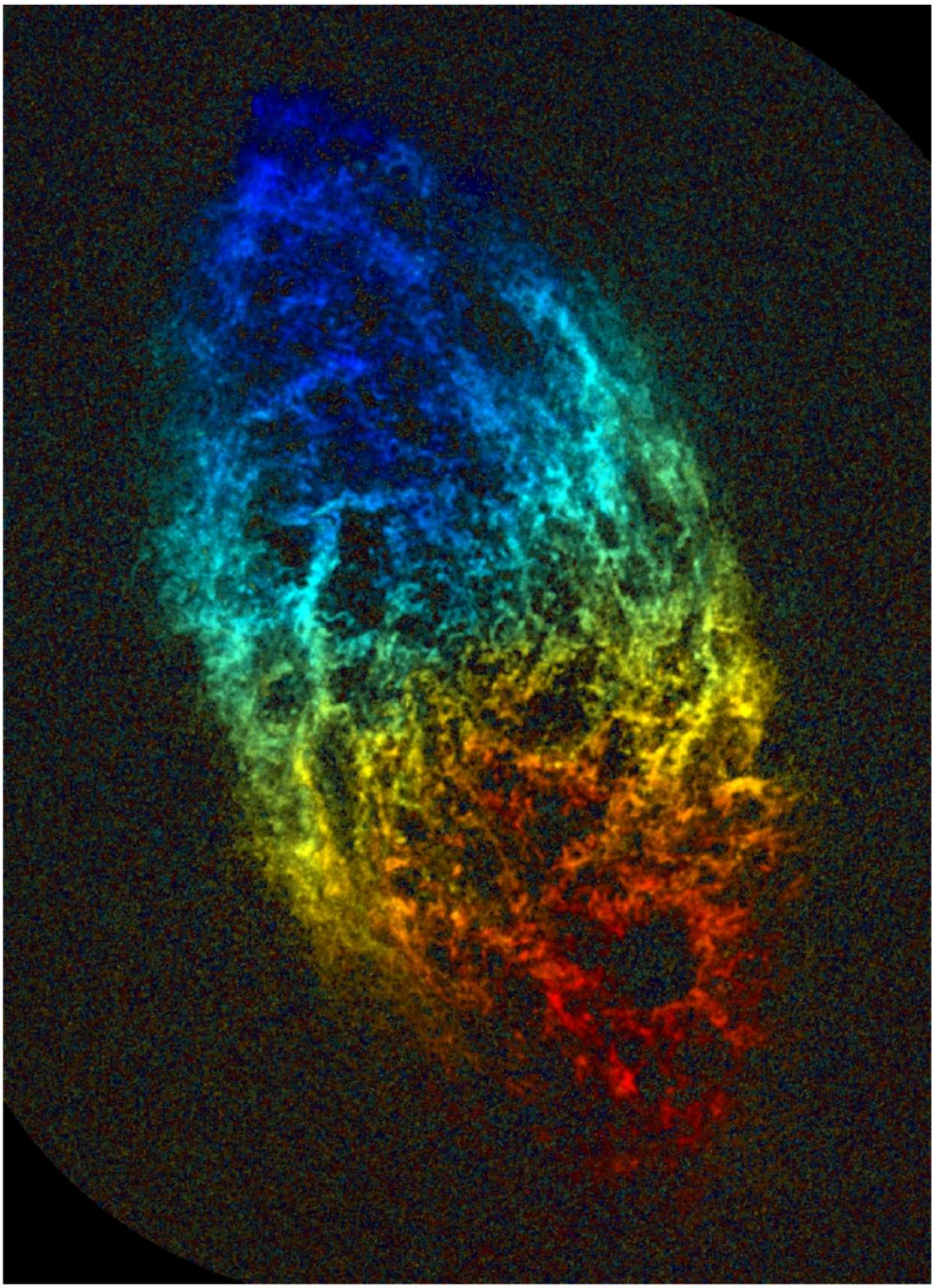

The HI radial velocity field of the nearby spiral galaxy M33 is shown here by colors corresponding to Doppler redshifts and blueshifts relative to the center of mass; brightness in this image is proportional to HI column density. Image credit

---

If the mass distribution of every galaxy were spherically symmetric, the gravitational force at radius r would equal the gravitational force of the enclosed mass $M(r)$. This is not a bad approximation, even for disk galaxies. Thus for gas in circular orbits,

$$\frac{GM}{r^2} = \frac{v^2}{r} ,$$

where M is the mass enclosed within the sphere of radius r and v is the orbital velocity at radius r, so

$$v^2 = \frac{GM}{r} .$$

Note that the velocity v is the full tangential velocity, not just the radial component $v_{\rm r}(r)$ that contributes to the observable Doppler shift:

$$v(r) = \frac{v_{\rm r}(r)}{\sin i} ,$$

where i is the inclination angle between the galaxy disk and the line-of-sight. The inclination angle of a thin circular disk can be estimated from the axial ratio

$$\cos i = \frac{\theta_{\rm m}}{\theta_{\rm M}} ,$$

where $\theta_{\rm m}$ and $\theta_{\rm M}$ are the minor- and major-axis angular diameters, respectively. Converting from cgs to astronomically convenient units yields

$$\left[\left(\frac{v}{\rm cm\ s^{-1}}\right)\left(\frac{10^5\ \rm cm\ s^{-1}}{\rm km\ s^{-1}}\right)\right]^2 =$$

$$\left[6.67\times10^{-8}\ \rm dyne\ cm^2\ g^{-2}\cdot\left(\frac{M}{\rm g}\right)\left(\frac{2\times10^{33}\ \rm g}{M_\odot}\right)\right]\left[\left(\frac{r}{\rm cm}\right)\left(\frac{3.09\times10^{21}\ \rm cm}{\rm kpc}\right)\right]^{-1}$$

$$10^{10}\left(\frac{v}{\rm km\ s^{-1}}\right)^2 = \left[6.67\times10^{-8}\cdot2\times10^{33}\left(\frac{M}{M_\odot}\right)\right]\left[3.09\times10^{21}\left(\frac{r}{\rm kpc}\right)\right]^{-1}$$

and we obtain the total galaxy mass inside radius r in units of the solar mass:

$$\left(\frac{M}{M_\odot}\right) \approx 2.3\times10^5\left(\frac{v}{\rm km\ s^{-1}}\right)^2\left(\frac{r}{\rm kpc}\right) \approx 2.3\times10^5\left[\frac{(v_{\rm r}/\sin i)}{\rm km\ s^{-1}}\right]^2\left(\frac{r}{\rm kpc}\right) \quad \text{(7E8)}$$

Example: What is the total mass of UGC 11707?

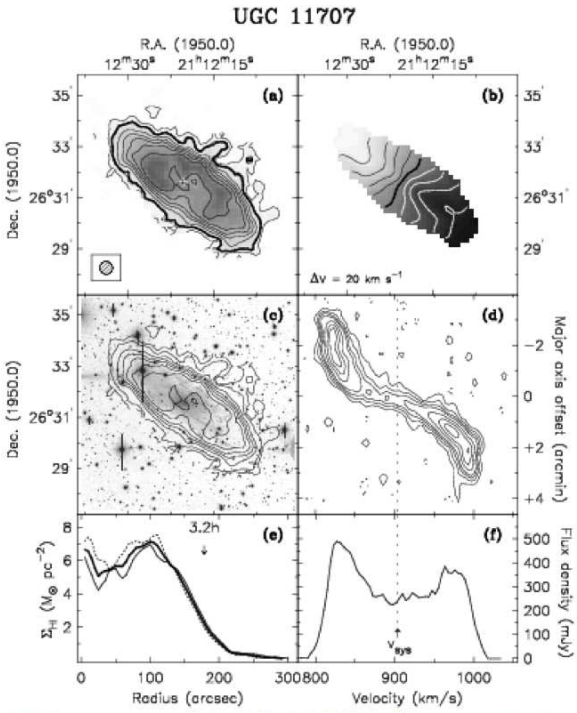

HI images of UGC 11707 (Swaters, R. A. et al. 2002, A&A, 390, 829). The contours in panels (a) and (c) outline the integrated HI brightness distribution. Panel (b) shows contours of constant velocity separated by 20 km s^{-1} and the darker shading indicates approaching gas. Panel (d) is a position-velocity diagram, panel (e) is the radial HI column-density profile, and panel (f) displays the integrated HI spectrum.

$$v_{\rm r} \approx \frac{\Delta v_{\rm r}}{2} \approx \frac{(1000\ {\rm km\ s^{-1}} - 800\ {\rm km\ s^{-1}})}{2} \approx 100\ {\rm km\ s^{-1}}$$

$$\cos i \approx \frac{\text{minor axis}}{\text{major axis}} \approx \frac{0.73 \times 10^{-3}\ {\rm rad}}{2.0 \times 10^{-3}\ {\rm rad}} \approx 0.365 \qquad \text{so} \qquad \sin i \approx 0.93$$

$$r \approx \theta_{1/2} D \approx 10^{-3}\ {\rm rad}\ \cdot 12.4\ {\rm Mpc} \approx 12.4\ {\rm kpc}$$

so

$$\left(\frac{M}{M_\odot}\right) \approx 2.3 \times 10^5 \cdot (100/0.93)^2 \cdot 12.4 = 3.3 \times 10^{10}\ .$$

UGC 11707 is a relatively low-mass spiral galaxy.

This "total" mass is really only the mass inside the radius sampled by detectable HI. Even though HI extends beyond most other tracers such as molecular gas or stars, it is clear from plots of HI rotation velocities versus radius that not all of the mass is being sampled, because we don't see the Keplerian relation $v_{\rm r} \propto r^{-1/2}$ which indicates that all of the mass is enclosed within radius r. Most ***rotation curves***, one-dimensional position-velocity diagrams along the major axis, are *flat* at large r, suggesting that the enclosed mass $M \propto r$ as far as we can see HI. The large total masses implied by HI rotation curves provided some of the earliest evidence for the existence of cold dark matter in galaxies.

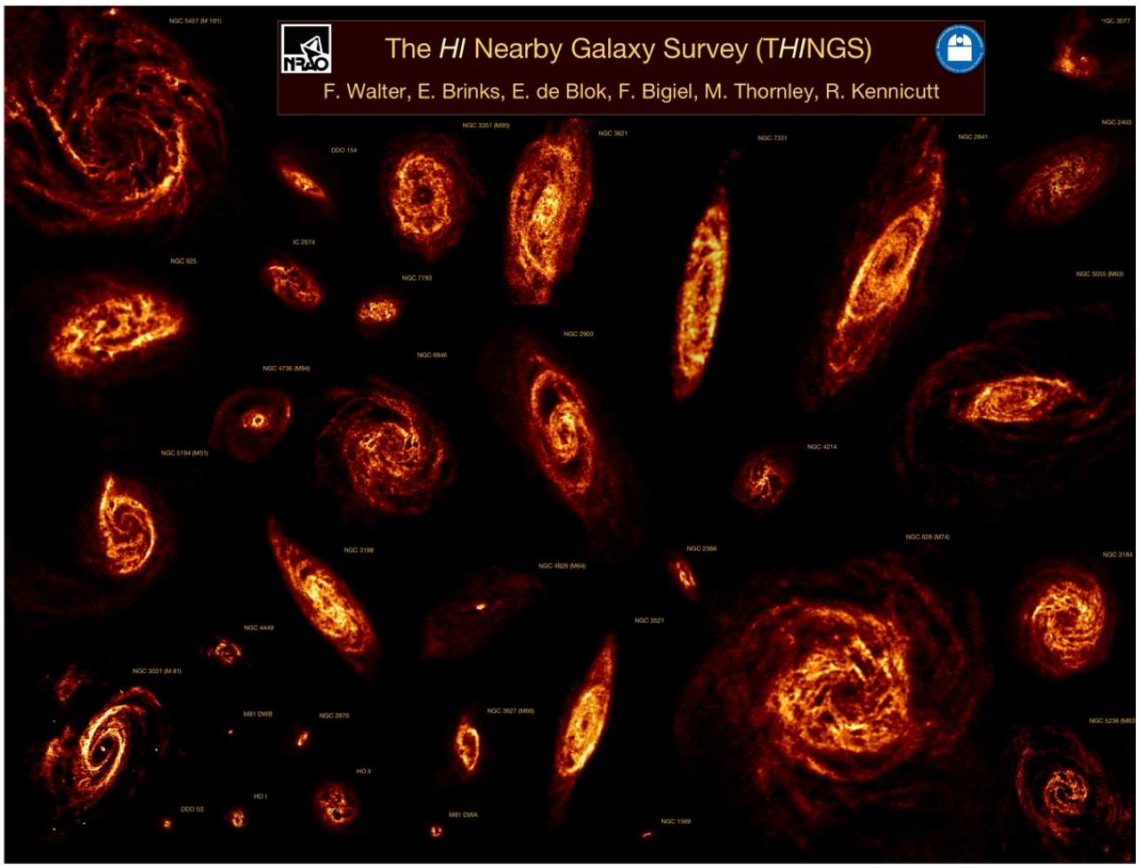

This poster shows VLA HI images of THINGS (The HI Survey of Nearby Galaxies) galaxies at constant linear scale and linear resolution. Image credit

---

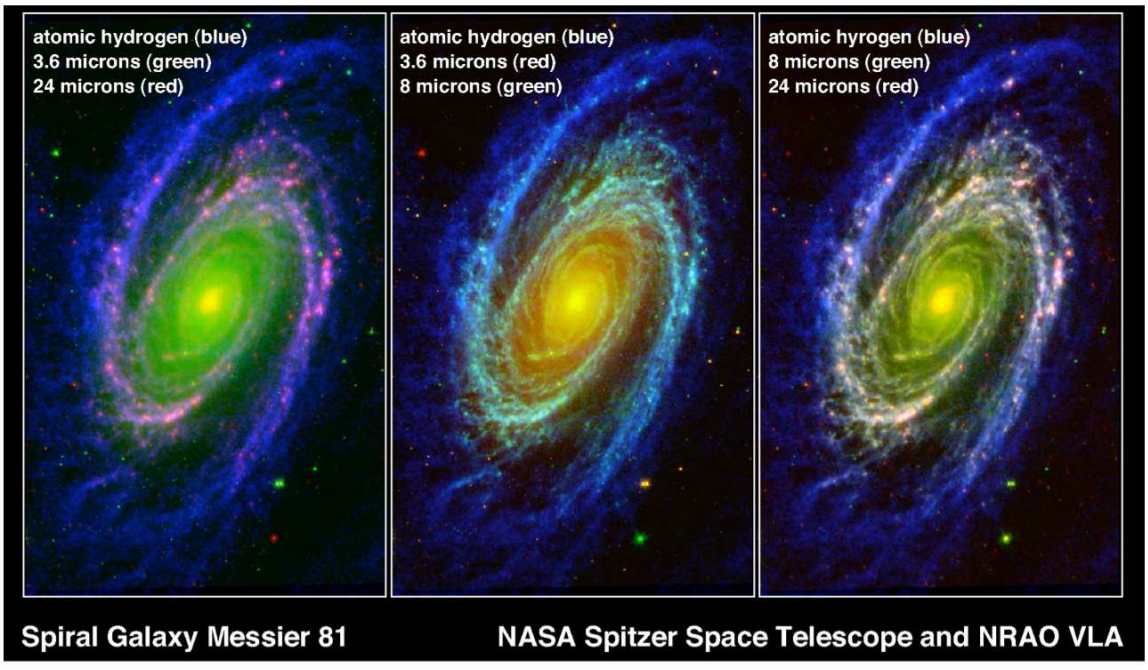

A high-resolution HI image of M81 made with the VLA for the THINGS (de Blok et al. 2007, astro-ph/0407103) survey compared with Spitzer mid-infrared emission.

Because detectable HI is so extensive, HI is an exceptionally sensitive tracer of tidal interactions between galaxies. Long streamers and tails of HI trace the interaction histories of pairs and groups of galaxies. See the HI Rogues Gallery for some spectacular examples.

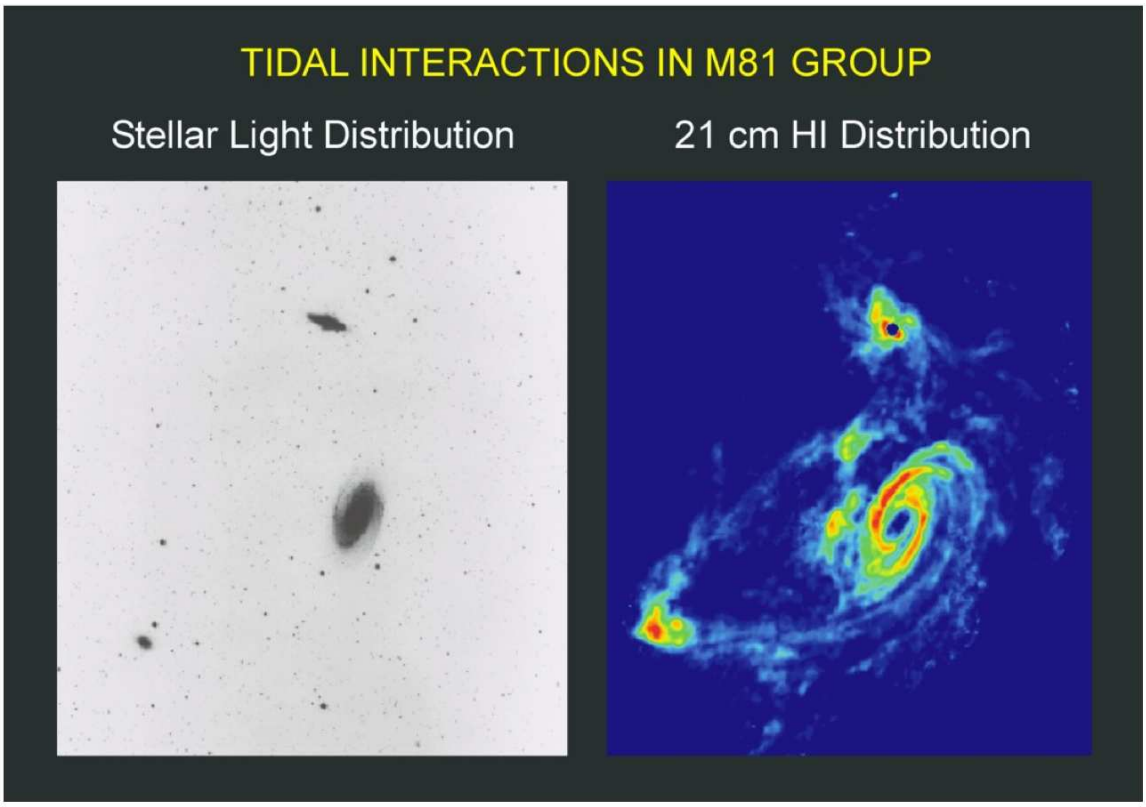

The streamers visible only in HI clearly demonstrate that the M81 group is an interacting system of galaxies. Image credit

---

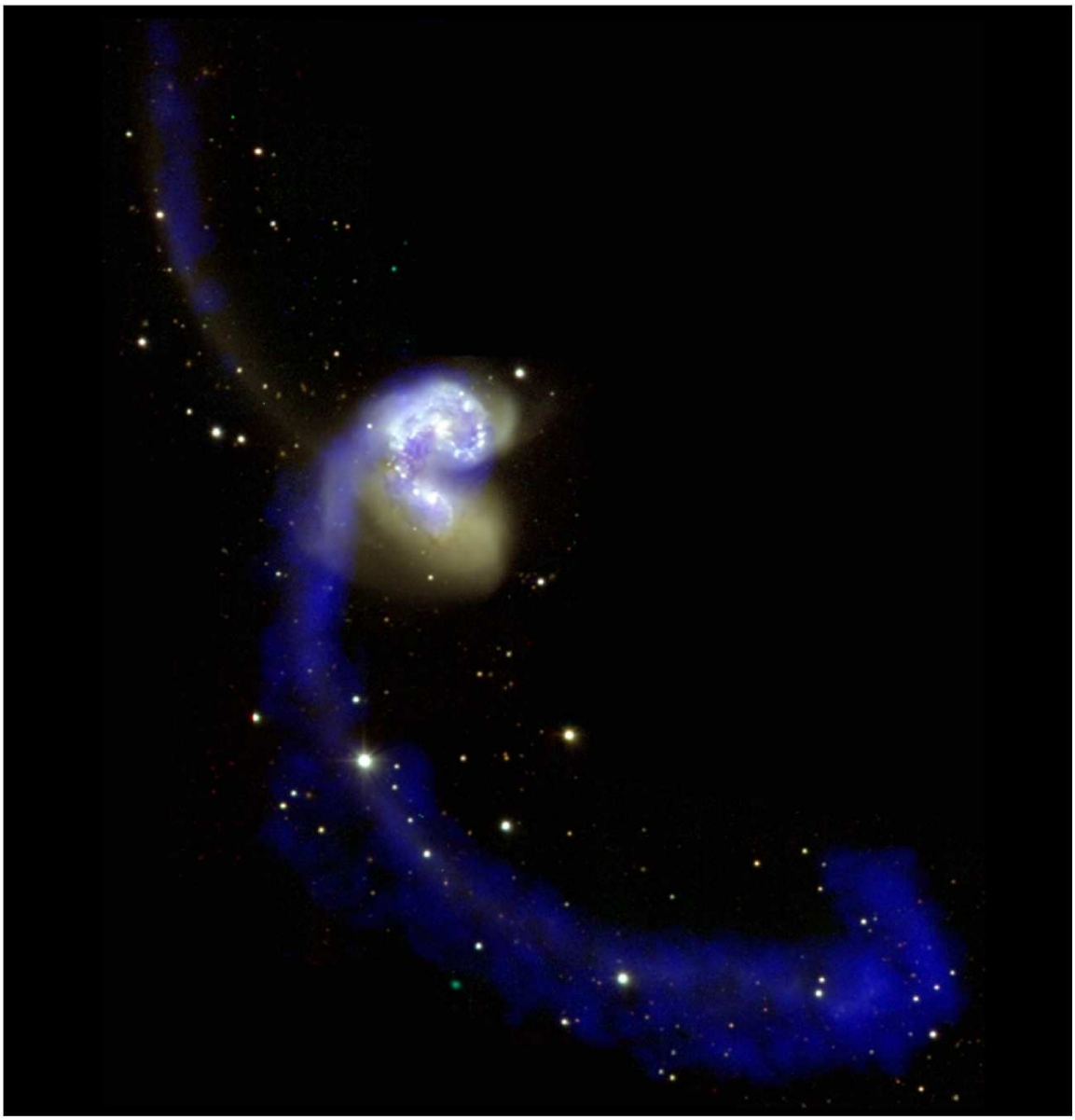

Optical (white) and HI (blue) images of the strongly interacting galaxies NGC 4038 and NGC 4039 (also known as the "antennae"). The velocity distributions of the long HI tidal tails provide strong constraints for computer models of the interaction history. Image credit

---

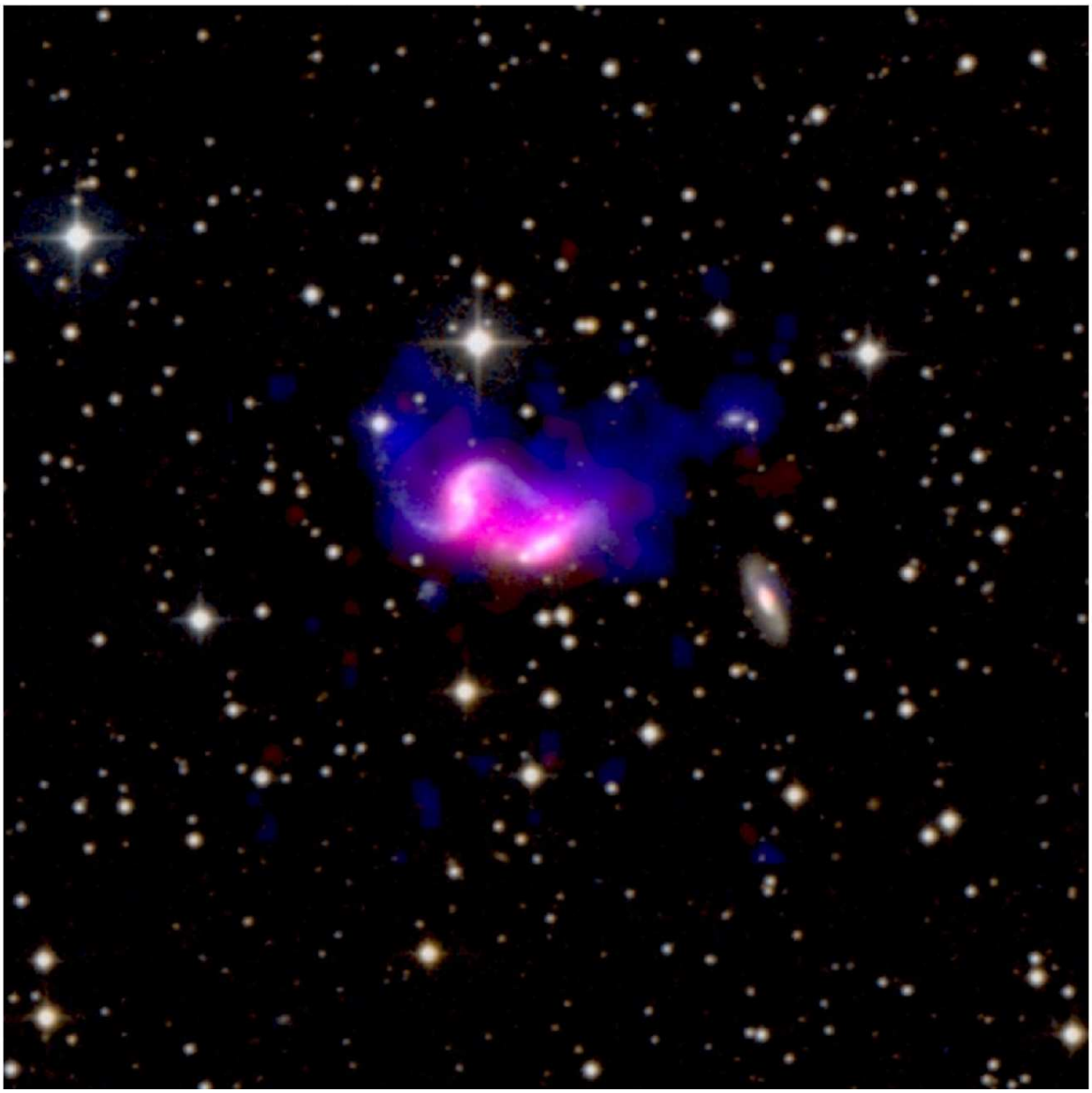

The radio continuum (red) and HI (blue) images of the post-merger pair of galaxies UGC 813 and UGC 816 indicate that the disks of these two galaxies passed through each other about 50 million years ago. Image credit

---

Another application of the HI spectra of galaxies is determining departures from smooth Hubble expansion in the local universe via the ***Tully-Fisher relation***. Most galaxies obey the empirical luminosity-velocity relation (Tully, R. B., & Fisher, J. R. 1977, A&A, 54, 661):

$$L \propto v_{\rm m}^4 \ ,$$

where $v_{\rm m}$ is the maximum rotation speed. Arguments based on the virial theorem can explain the Tully-Fisher relation if all galaxies have same central mass density and density profile, differing only in scale length, and also have the same mass-to-light ratio. Thus a measurement of $v_{\rm m}$ yields an estimate of L that is independent of the Hubble distance $D_{\rm H}$. The Tully-Fisher distance $D_{\rm TF}$ can be calculated from this "standard candle" L and the apparent luminosity. Apparent luminosities in the near infrared ($\lambda \sim 2\,\mu$m) are favored because the near-infrared mass-to-light ratio of stars is nearly constant and independent of the star-formation history, and because extinction by dust is much less than at optical wavelengths. Differences between $D_{\rm TF}$ and $D_{\rm H}$ are ascribed to the ***peculiar velocities*** of galaxies caused by intergalactic gravitational interactions. The magnitudes and scale lengths of the peculiar velocity distributions are indications of the average density and clumpiness of mass on megaparsec scales.

Large-Scale Structure

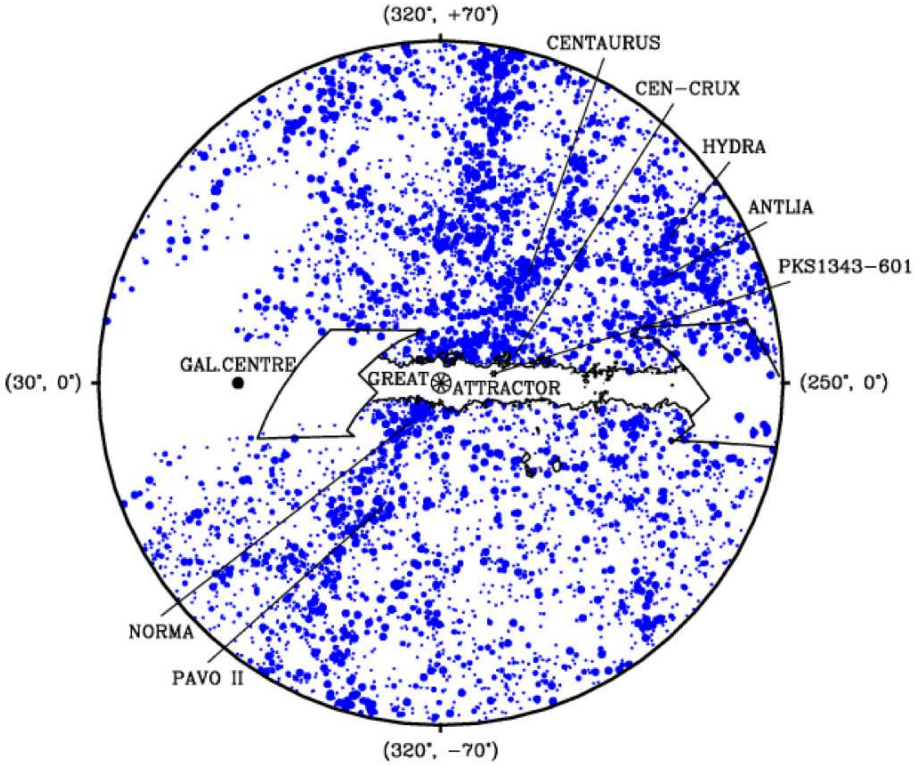

The Great Attractor.

Baryon Acoustic Oscillations

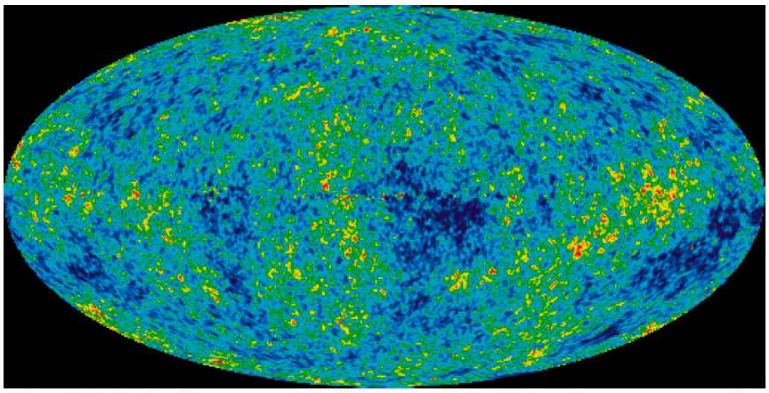

The WMAP five-year all-sky the CMB. Image credit

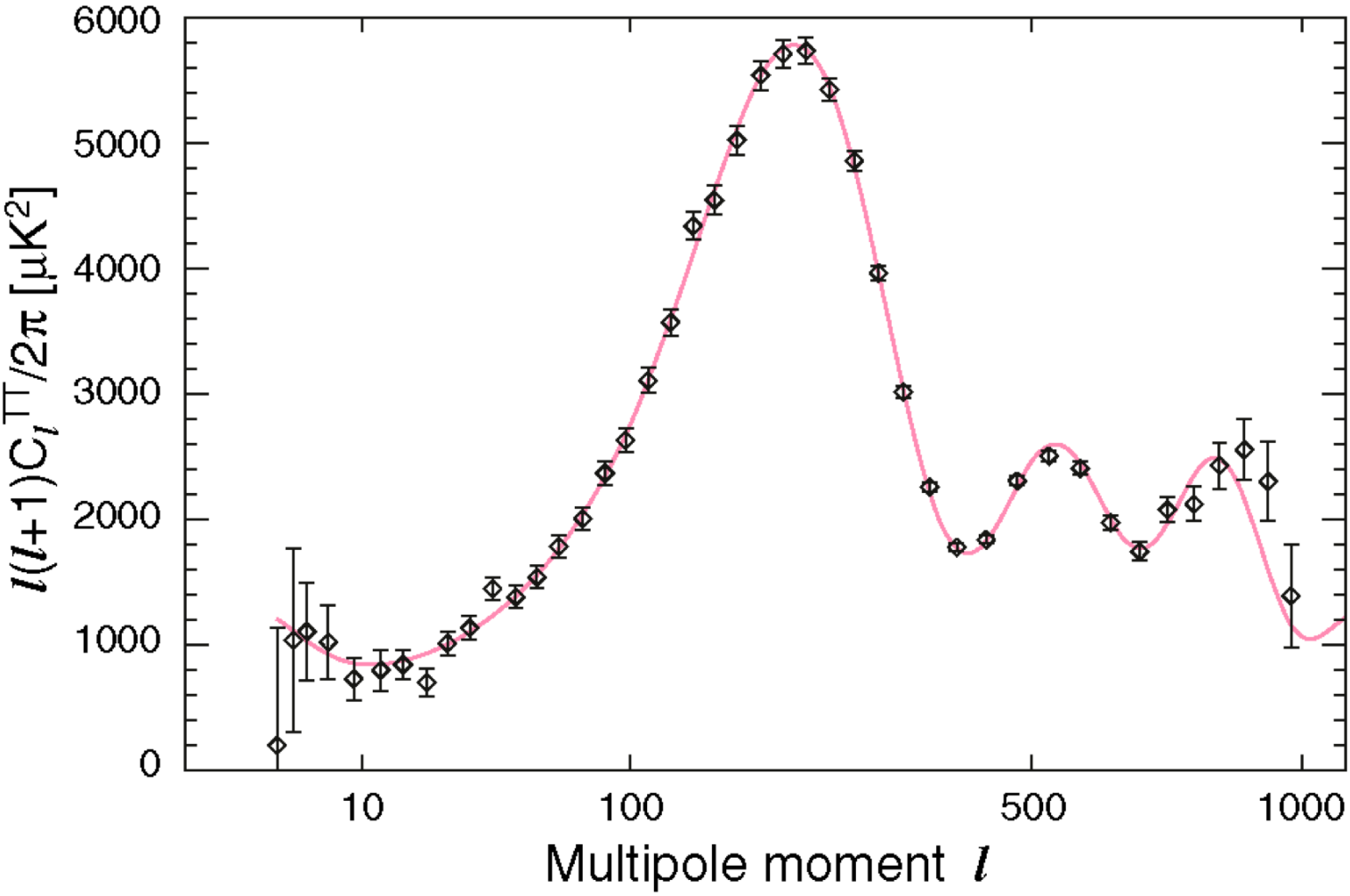

The WMAP five-year power spectrum of the CMB. [Image credit]

Epoch of Reionization (EOR)

Most of the normal matter in the early universe was fully ionized hydrogen and helium gas, plus trace amounts of heavier elements. This smoothly distributed gas cooled as the universe expanded, and the free protons and electrons recombined to form neutral hydrogen at a redshift $z \approx 1091$ when the age of the universe was about 3.8×10^5 years. The hydrogen remained neutral during the "dark ages" prior to the formation of the first ionizing astronomical sources, massive ($M > 100 M_\odot$) stars, galaxies, quasars, and clusters of galaxies, by gravitational collapse of overdense regions. These astronomical sources gradually started reionizing the universe when it was several hundred million years old ($z \sim 10$) and completely reionized the universe by the time it was about 10^9 years old ($z \sim 6$). This era is called the ***epoch of reionization***.

The highly redshift HI signal was uniform prior to the first reionization. The signal developed structure on angular scales up to several arcmin as the first sources created bubbles of ionized hydrogen around them. As the bubbles grew and merged, the HI signal developed frequency structure corresponding to the redshifted HI line frequency. The characteristic size of the larger bubbles reached about 10 Mpc at $z \sim 6$, corrresponding to HI signals having angular scales of several arcmin and covering frequency ranges of several MHz. These the HI signals encode unique information about the formation of the earliest astronomical sources.

The HI signals produced by the EOR will be very difficult to detect because they are weak (tens of mK), relatively broad in frequency, redshifted to low frequencies (< 200 MHz) plagued by radio-frequency interference, and lie behind a much brighter (tens of K) foreground of extragalactic continuum radio sources. Nonetheless, the potential scientific payoff is so great that several groups

around the world are developing instruments to detect the HI signature of the EOR. One such instrument is the Precision Array to Probe the Epoch of Reionization (PAPER), a joint project of UC Berkeley, the NRAO, and the University of Virginia that has placed a test array in Green Bank, WV and will soon construct a science array in western Australia, where there is very little RFI.